

Discovery of a Potent and Selective Naphthyridine-based Chemical Probe for Casein Kinase 2

Zachary W. Davis-Gilbert¹, Andreas Krämer^{2,3,4}, James E. Dunford⁵, Stefanie Howell¹, Filiz Senbabaoglu⁵, Carrow I. Wells¹, Tammy M. Havener¹, Jeffery L. Smith¹, Mohammad A. Hossain¹, Udo Oppermann^{5,6}, David H. Drewry^{1,7}, Alison D. Axtman^{*,1}

¹ Structural Genomics Consortium, UNC Eshelman School of Pharmacy, University of North Carolina at Chapel Hill, Chapel Hill, NC, 27599, USA

² Institute of Pharmaceutical Chemistry, Goethe University Frankfurt, Max-von-Laue-Strabe 9, Frankfurt 60438, Germany

³ Structural Genomics Consortium, Buchmann Institute for Life Sciences, Goethe University Frankfurt, Max-von-Laue-Strabe 15, Frankfurt 60438, Germany

⁴ Frankfurt Cancer Institute, Paul-Ehrlich-Straße 42-44, Frankfurt 60596, Germany

⁵ Botnar Research Centre, Nuffield Department of Orthopaedics, Rheumatology and Musculoskeletal Sciences, University of Oxford, OX3 7LD, United Kingdom

⁶ Oxford Translational Myeloma Centre, University of Oxford, OX3 7LD, United Kingdom

⁷ UNC Lineberger Comprehensive Cancer Center, School of Medicine, University of North Carolina at Chapel Hill, Chapel Hill, NC, 27599, USA

ABSTRACT

Naphthyridine-based inhibitors were synthesized to yield a potent and cell-active inhibitor of casein kinase 2 (CK2). Compound **2** selectively inhibits CK2 α and CK2 α' when profiled broadly, making it an exquisitely selective chemical probe for CK2. A negative control that is structurally related but lacks a key hinge-binding nitrogen (**7**) was designed based on structural studies. Compound **7** does not bind CK2 α or CK2 α' in cells and demonstrates excellent kinome-wide selectivity. Differential anti-cancer activity was observed when compound **2** was profiled alongside a structurally distinct CK2 chemical probe: SGC-CK2-1. This naphthyridine-based chemical probe (**2**) represents one of the best available small molecule tools to interrogate biology mediated by CK2.

KEYWORDS: casein kinase 2, CK2, CSNK2, protein kinase, naphthyridine, chemical probe

Casein kinase 2 (CK2, CSNK2) is a highly conserved and ubiquitously expressed serine/threonine kinase for which more than 300 substrates have been identified and, correspondingly, many diverse functions and roles in disease have been ascribed to CK2.¹⁻⁵ Examples of indications for which CK2 inhibition has been investigated as therapeutically beneficial include cancer, SARS-CoV-2, and neuroinflammation.⁶⁻¹⁰ Since the two catalytic subunits of CK2, CK2 α (encoded by the CSNK2A1 gene) and CK2 α' (encoded by the CSNK2A2 gene), have >80% identity, small molecule inhibitors bind to both.^{11, 12} As confirmed via western blot analyses, inhibitor binding to the two catalytic subunits in cells results in

inhibition of the heterotetrameric holoenzyme, which includes a dimer of noncatalytic subunits (CK2 β).¹¹⁻¹³

Recent efforts have identified potent and selective tool molecules that enable the dissection of complex signaling pathways mediated by CK2: IC19, IC20, and SGC-CK2-1 (Figure 1).^{11, 12} Naphthyridine-based CK2 inhibitors were first described in 2010.^{14, 15} The most widely used and advanced compound from this series, CX-4945 (silmittasertib), has been evaluated clinically for several oncology indications and recently for SARS-CoV-2.^{6, 16} Silmittasertib received orphan drug status in the United States for the treatment of advanced cholangiocarcinoma.^{9, 10} CX-4945 inhibits a number of kinases in addition to CK2, raising the possibility that its success in cancer models may be due, at least in part, to polypharmacology.^{11, 16} Efforts aimed at narrowing the inhibition profile of CX-4945 have resulted in several naphthyridine analogs, including CX-5011, CX-5279, and CX-5033 (Figure 1), that demonstrate improved selectivity when compared to CX-4945.^{11, 17}

The clinical promise of the naphthyridine scaffold, demonstrated by the advancement of silmittasertib to Phase II clinical trials in addition to its acceptable human oral bioavailability,

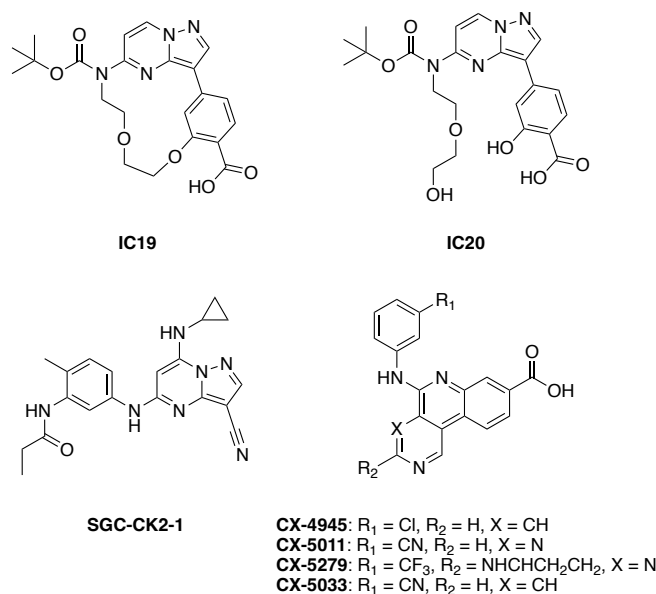


Figure 1. Structures of literature reported potent CK2 inhibitors.

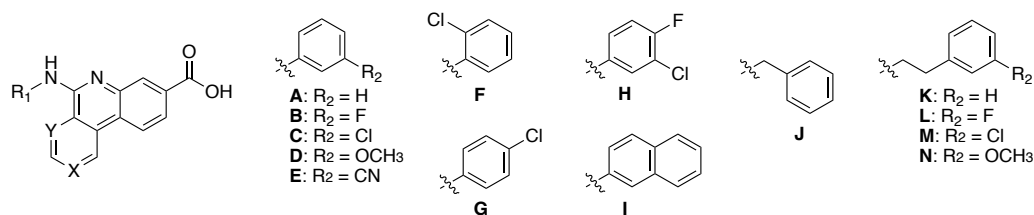
motivated further exploration of this chemotype. Despite reports of multiple exemplified naphthyridine analogs with nanomolar biochemical potency for CK2 and antiproliferative activity, a chemical probe with kinome-wide selectivity has not been described based upon this core.^{16, 17} Such a compound would represent an orthogonal tool that would aid in deciphering the complex biological roles of CK2. We hypothesized that synthesizing and characterizing naphthyridine analogs would allow for discovery of a potent and selective tool in this chemical class.

To complement the data that has been collected for published analogs and expand knowledge around this chemotype, we prepared a series of naphthyridines. We chose to explore the R₁ position in addition to the presence or absence of the nitrogens in the fused ring system. As shown in Table 1, either a pyridine or pyrimidine was appended to the quinoline core to form the tricyclic system found in CX-4945/CX-5033 or CX-5011/CX-5279, respectively. These compounds were evaluated in the CK2 α and CK2 α' NanoBRET assays to gauge their ability to engage the target kinase CK2 in cells. Most CK2 NanoBRET assays were run in triplicate (Figures 2, 3, S1, and S2). The NanoBRET data revealed that molecules from this series engaged CK2 α' and CK2 α with IC₅₀ values of generally less than 1 μ M. Excluding CX-4945, a pronounced 2.3–13-fold bias was observed when comparing IC₅₀ values for CK2 α' to those for CK2 α . Previously reported CK2 NanoBRET IC₅₀ values for CX-4945 align with this trend (7.6-fold bias).¹¹ Compound **18** demonstrated the most significant difference in IC₅₀ values. A more modest 2.3-fold bias for CK2 α' versus CK2 α was observed for SGC-CK2-1 and was consistent in the pyrazolopyrimidine series from which it was selected.¹¹ Compound **11** was the

most potent compound in both CK2 NanoBRET assays ($IC_{50} < 22$ nM), while CX-5033 was weakest in these assays ($IC_{50} > 1800$ nM).

Given the published off-targets of CX-4945, the selectivity of these CK2-targeting compounds was important to assess, especially against the highly homologous CMGC kinases from the DYRK and HIPK sub-families, which share many key active site residues with CK α and CK2 α' . Enzymatic activity assays were carried out at a single concentration (1 μ M) of inhibitor to generate percent of control (PoC) values (Table S1). Several compounds, including compounds **2**, **8**, **9**, and **21**, lacked activity against DYRKs and HIPKs, while a few others, including compounds **10**, **17**, **18**, and **24**, demonstrated potent inhibition of just one kinase in the 8-member panel. This result reinforced the idea that selectivity can be imparted in the naphthyridine scaffold. Most compounds (11 in total), however, potently inhibited more than half of the kinases in this enzymatic panel. While it is not a direct comparison, CX-4945 exhibits PoC <10 for all of these same kinases in Table S1 when profiled in the DiscoverX *scanMAX* panel at 1 μ M (minus DYRK3 since it is not included in the *scanMAX* panel).¹¹ In our limited DYRK and HIPK sub-family panel, more kinases preferred naphthyridine analogs with Y = CH versus Y = N (Table 1), rendering them generally less selective.

Table 1. Potency and selectivity data for naphthyridine library.



Compound	NanoBRET data				Selectivity data		
	X	Y	R ₁	CK2 α IC ₅₀ (nM)	CK2 α' IC ₅₀ (nM)	S ₁₀ (1 μ M) score	# kinases with PoC <10
2	N	N	J	920	200	0.007	3
8	N	N	N	570	93	0.017	7
9	N	N	M	830	140	0.02	8
10	N	N	L	930	270	0.022	9
11	N	N	I	21	6.0	0.025	10
12	N	N	G	240	25	0.032	13
13	N	N	B	350	51	0.042	17
14	N	N	H	110	19		
15	N	N	F	300	42		
16	N	N	A	740	63		
17	N	N	K	550	110		
CX-5011	N	N	E	350	66		
18	N	CH	M	230	17	0.035	14
19	N	CH	G	430	130	0.05	20
CX-5033	N	CH	E	4300	1900	0.079	32
20	N	CH	I	100	22		
21	N	CH	J	1100	450		
22	N	CH	L	300	62		
23	N	CH	B	680	180		
24	N	CH	N	150	19		
25	N	CH	A	1400	420		
26	N	CH	H	220	43		
27	N	CH	K	260	34		
28	N	CH	D	1200	340		
CX-4945	N	CH	C	240	180	0.069	28
7	CH	N	J	>10000	>10000	0	0

$S_{10}(1 \mu\text{M})$: percentage of screened kinases with PoC <10 at 1 μM ; PoC: percent of control values determined at 1 μM via DiscoverX *scanMAX* profiling.

We considered both the CK2 NanoBRET potency and the small panel enzymatic results to select some analogs for DiscoverX *scanMAX* profiling. This kinome-wide profiling was executed at a single inhibitor concentration (1 μM). DiscoverX *scanMAX* data previously generated for CX-4945 is included in Table 1, showing it has an $S_{10} = 0.069$ and that it potently binds to nearly 7% of the wild-type human kinases in the panel.¹¹ Compound **14** was chosen based on its potency for CK2 α and CK2 α' in the corresponding NanoBRET assays (Table 1). Compounds **2**, **8**, **9**, **10** and **18** were also profiled based upon their potent inhibition of 1 or fewer kinases in the enzymatic panel (Table S1). Finally, compounds **12**, **13**, **19**, and CX-5033 were selected as potent inhibitors of HIPK2 with or without CK2 affinity. Exemplars with Y = CH and Y = N (Table 1) were included to determine if the selectivity trend in Table S1 was maintained when more kinases were sampled. The kinome-wide profiling data summarized in the $S_{10}(1 \mu\text{M})$ column of Table 1 supports the trend of overall selectivity improvements for the Y = N versus Y = CH compounds. Specific examples include compounds **9** versus **18** and **12** versus **19** where the analog bearing Y = N demonstrated a better selectivity score. Except for CX-5033, all compounds demonstrated an improved selectivity score when compared to CX-4945. Compound **2** emerged as the most promising compound when considering broad selectivity ($S_{10}(1 \mu\text{M}) = 0.007$).

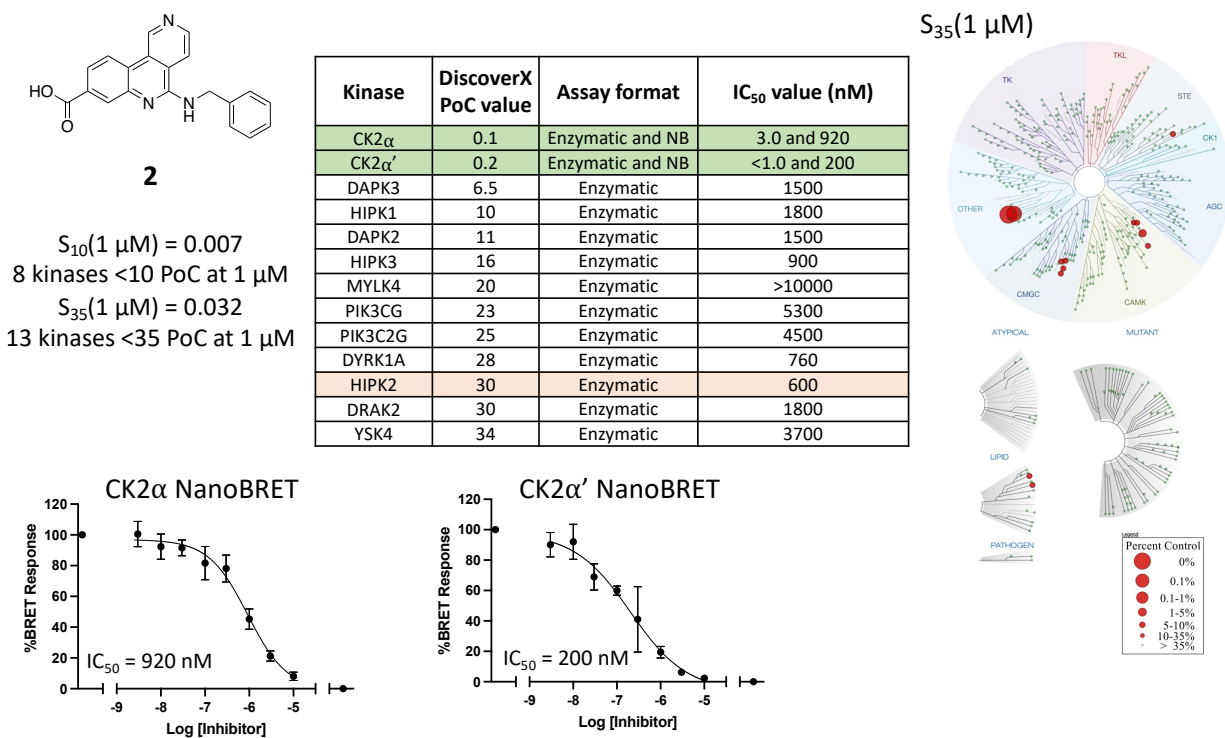


Figure 2. Structure, potency, and selectivity data related to CK2 chemical probe **2**. Kinome tree shows kinases that bind with PoC <35 when compound **2** was screened at 1 μM . Assay format used to generate data in the last column of nested table is listed in the preceding column. CK2 NanoBRET assays run in triplicate ($n = 3$), error bars represent standard deviation (SD). PoC = percent of control; NB = NanoBRET.

A deeper dive into the DiscoverX *scanMAX* data generated for compound **2** revealed 13 kinases with PoC <35, including CK2 α and CK2 α' (Figure 2). Enzymatic assays were employed as an orthogonal method to validate the *scanMAX* binding data for these 13 kinases. Potent

inhibition of CK2 α and CK2 α' was observed ($IC_{50} \leq 3$ nM). Furthermore, the exquisite selectivity of compound **2** was confirmed as a 200-fold window between inhibition of CK2 α and HIPK2, the next most potently inhibited kinase ($IC_{50} = 600$ nM), was noted. This compound demonstrates a 4.6-fold bias for binding CK2 α' versus CK2 α in the corresponding NanoBRET assays (Table 1) and a similar trend in CK2 enzymatic assays (Figure 2).

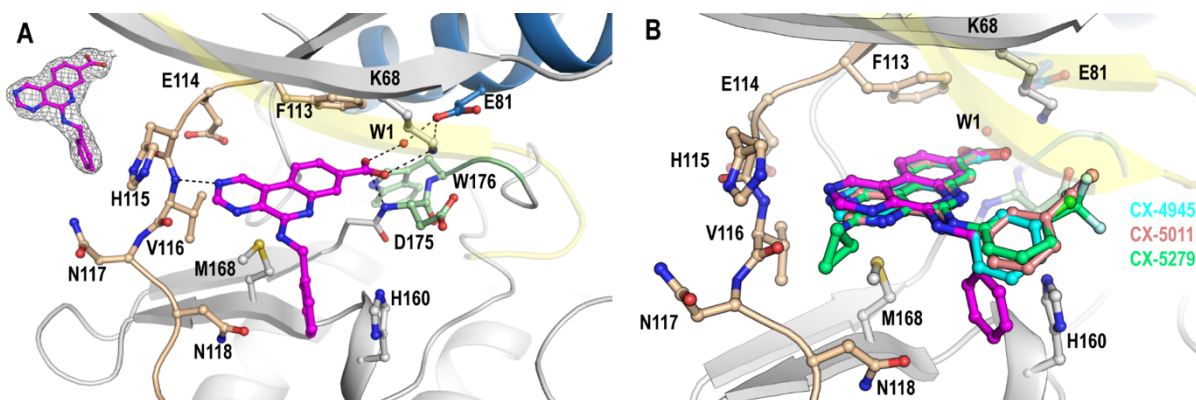


Figure 3. (A) Crystal structures of human CK2 α in complex with compound **2** (pink) in cartoon (CK2 α) and stick (compound **2**) representation. The hinge region is colored in wheat, the α C helix blue, the DWG motif green, and water molecule is shown as red sphere. The P-loop in yellow was made transparent for better view of the interactions. Hydrogen bonds are indicated as black dashed lines. The insert on the upper left corner the electron density map ($2F_o - F_c$) of the bound ligand contoured at 1σ . (B) Overlay of compound **2** with published naphthyridine analogs (PDB codes 3NGA, 3PE2, 3ROT) in the same color scheme as panel A.

Structural studies were employed to rationalize the selectivity of compound **2** for CK2. A co-crystal structure of compound **2** bound to CK2 α was solved (Figure 3A, Table S2). This structure confirmed a key hydrogen bond between the nitrogen at the ‘X’ position in Table 1 and a backbone NH between H115 and V116. Additional hydrogen bonds were noted between the carboxylic acid and K68, a water mediated with E81 on the α C helix, and a backbone NH adjacent to D175 from the DWG motif. This binding mode was compared with those previously solved for CX-4945, CX-5011, and CX-5279 (Figure 3B). The main difference observed was the orientation of the pendant aryl ring in the front pocket. Compound **2**, which is shown in pink in panel B, can form an additional π -stacking interaction with H160 that is absent in previously solved structures. The methylene spacer present in compound **2**, but not in the other scaffolds where the aryl ring is directly attached, positions the aryl ring so that it can adopt this favorable conformation. It is likely that the ATP binding sites of other kinases do not accommodate this ring in the same way, precluding their binding to compound **2** with high affinity and imparting the selectivity we observe. Many more kinases tolerate binding of naphthyridine analogs with the aryl ring directly attached, including compounds **11**, **12**, **13**, **19**, CX-5033, and CX-4945 in Table 1 that all bind 10 or more kinases with PoC < 10 . While the single methylene unit seems to provide the most optimal ability to π -stack, compounds **8**, **9**, **10**, and **18** in Table 1 demonstrate that the incorporation of two methylene groups between the core and pendant aryl ring also imparts selectivity versus those analogs with the aryl ring directly attached.

Consideration of the naphthyridine co-crystal structures (Figure 3) aided in design of an appropriate negative control compound to be used alongside compound **2** in a chemical probe set. To synthesize a structurally related compound that lacked an ability to bind to CK2, we targeted the hinge-binding nitrogen specifically. Compound **7** was prepared with the ‘X’ position in Table 1 replaced by a carbon. The resulting compound was evaluated in the CK2 α and CK2 α' NanoBRET assays, where it was found to not bind either kinase at concentrations up to 10 μ M

(Table 1 and Figure 4). When profiled in the DiscoverX *scanMAX* panel at 1 μM , a single kinase (PIP5K1C) bound with PoC <35. Enzymatic follow-up, however, demonstrated that this binding in the DiscoverX panel did not result in PIP5K1C inhibition. Thus, modification of the hinge-binding atom on compound **2** resulted in a negative control (**7**) that lacks CK2 and kinome-wide binding.

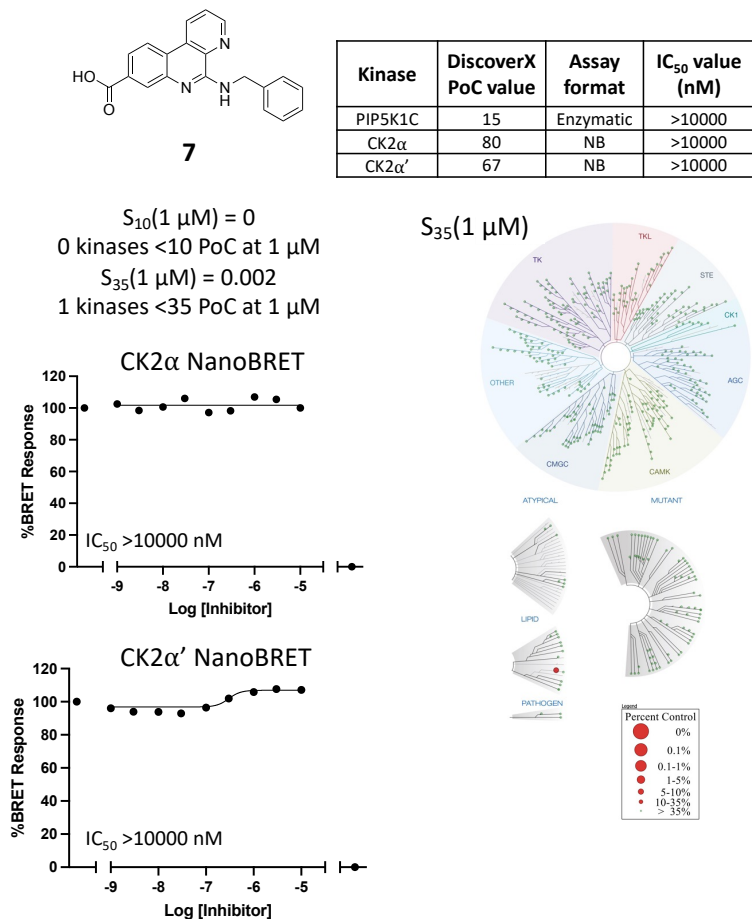


Figure 4. Structure, potency, and selectivity data related to CK2 negative control **7**. Kinome tree shows kinases that bind with PoC <35 when compound **7** was screened at 1 μM . Assay format used to generate data in the last column of nested table is listed in the preceding column. CK2 NanoBRET assays run in singlicate ($n = 1$). PoC = percent of control; NB = NanoBRET.

(NanoBRET IC₅₀ values of 16–36 nM for SGC-CK2-1 and 200–920 nM for compound **2**).¹¹ This result confirmed that CK2 inhibition by compound **2** disrupts CK2-mediated downstream signaling.

Neither compound **2** nor SGC-CK2-1 exhibited significant cytotoxicity when MDA-MB-231 cells were treated for 48 hours up to a concentration of 10 μM (Figure S3). Compounds **7**, CX-5011, and CX-4945 similarly did not exhibit cytotoxicity in our study (Figure S3). There are several possible explanations for the discrepancy between our observed lack of impact of naphthyridine compounds on viability and their published effect on cell growth.¹⁸ It has been reported that when treated with micromolar concentrations (2–10 μM) of CX-4945 for 24–72 hours, MDA-MB-231 cell growth is inhibited. The authors point out that they rely on a WST-1 assay for readout and this indirectly measures cell growth based upon metabolic activity in the

With a potent and selective compound in hand, we evaluated the impact on downstream signaling in response to compound **2**. In a previous report, CX-4945 was found to reduce viability, induce cell cycle arrest and apoptosis, and hamper migratory capacity of MDA-MB-231 cells, a triple negative breast cancer cell line with elevated CK2 expression.¹⁸ This result motivated examination of the response of MDA-MB-231 cells to treatment with compound **2**. An orthogonal CK2 probe known to inhibit downstream signaling mediated by CK2, SGC-CK2-1 (Figure 1), was included in these experiments. As shown in Figure 5, 24h exposure of MDA-MB-231 cells to either SGC-CK2-1 or compound **2** resulted in dose-dependent inhibition of AKT phosphorylation with no impact on total AKT expression. The concentration at which AKT phosphorylation is inhibited by each compound corresponds well with their respective IC₅₀ values in the CK2 NanoBRET assays

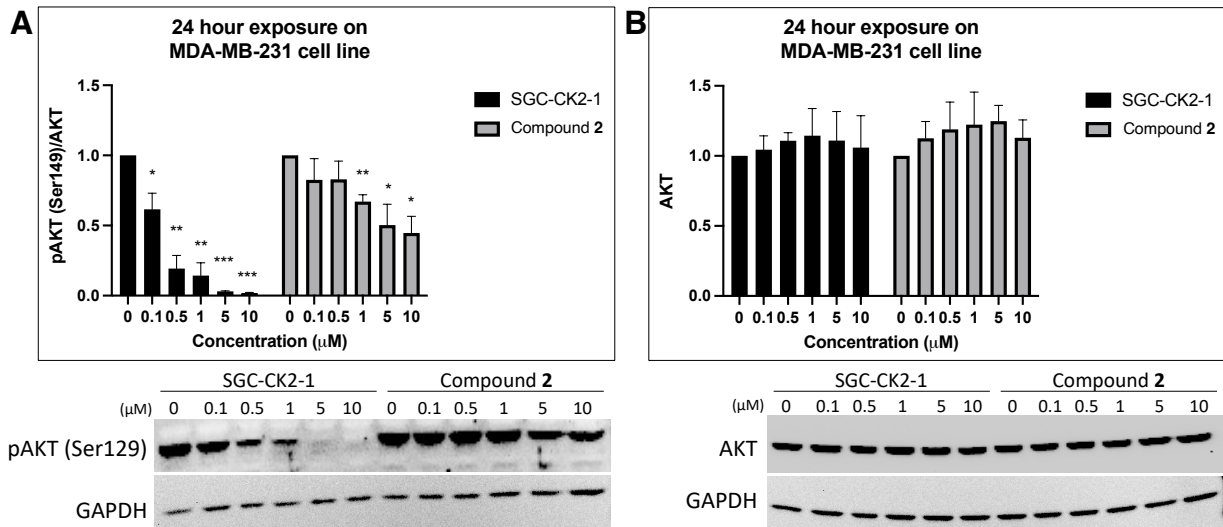


Figure 5. (A) Western blot analyses of pAKT in MDA-MB-231 cells after 24 h treatment with SGC-CK2-1 or compound 2. Representative blot and quantification of phospho-AKT (Ser129) normalized to AKT, $n = 3$. SGC-CK2-1 p-values: 0.1 $\mu\text{M} = 0.0287$, 0.5 $\mu\text{M} = 0.0045$, 1 $\mu\text{M} = 0.0038$, 5 $\mu\text{M} < 0.0001$, 10 $\mu\text{M} < 0.0001$. Compound 2 p-values: 1 $\mu\text{M} = 0.0072$, 5 $\mu\text{M} = 0.0286$, 10 $\mu\text{M} = 0.0149$. (B) Western blot analyses of pAKT in MDA-MB-231 cells after 24 h treatment with SGC-CK2-1 or compound 2. Representative blot and quantification of total AKT, $n = 3$. Error bars represent SEM. P-values were generated using a parametric unpaired t-test with Welch's correction comparing each treatment condition to the untreated control.

cells.¹⁸ CK2 regulates cell metabolism, which is a process that can be inhibited without an associated impact on cell growth.^{1, 19} Another potential explanation is that MDA-MB-231 cells are moderately sensitive to the promotion of CK2-independent cytoplasmic vacuolization, called methuosis, at micromolar concentrations of CX-4945 and CX-5011.²⁰⁻²² Metabolic-based viability assay (MTT) results generated in parallel support the idea that this vacuolization impacts cell metabolism.²⁰ Similarly, methuosis is reported to drive metabolic failure.²³ In contrast to an assay dependent on mitochondrial enzymes (WST-1), we opted to employ a luciferase-based assay (CellTiter-Glo2) that requires ATP in order to generate the luminescent species.

CK2 has been recognized as an essential mediator in hematological malignancies.^{10, 24} Multiple myeloma cells have been reported to rely on elevated CK2 for survival. Accordingly, when CX-4945 was profiled against a panel of 13 multiple myeloma cell lines, low micromolar antiproliferative activity was measured via a CellTiter-Glo viability assay.²⁵ CX-4945 has been explored clinically for relapsed or refractory multiple myeloma.¹⁰ Apoptosis was induced in multiple myeloma cells from patients when treated with orthogonal CK2 inhibitors (TBB, a TBB derivative, or CGP029482), much more effectively than in nonmalignant control cells.^{26, 27} This data motivated our examination of the effect of compound 2 versus published naphthyridines (CX-4945, CX-5011, and CX-5033) and SGC-CK2-1 at a single, preliminary concentration of 1 μM on a panel of multiple myeloma cell lines. The response of JLN3, AMO-1 (parental and pomalidomide-resistant), and L363 (parental, carfilzomib-resistant, and bortezomib-resistant) multiple myeloma cell lines to treatment was analyzed via a metabolic-based viability assay using resazurin. As shown in Figure 6A, our preliminary data demonstrates that JLN3 cells were not responsive to treatment with any compound. The viability of AMO-1 and L363 parental lines was reduced by treatment with compound 2, but not by treatment with the other naphthyridine analogs. We observed 44% viability of AMO-1 and 36% viability of L363 cells, respectively, following treatment with 1 μM of compound 2. Viability of AMO-1 and L363 drug-resistant lines was not impacted by treatment with any naphthyridine analog. Interestingly, the viability of

all AMO-1 and L363 cell lines tested was significantly compromised by treatment with 1 μ M of SGC-CK2-1, resulting in 9–22% viability of AMO-1 and L363 cells and 77% viability of JJN3 cells. This suggests a chemotype-specific response and/or reflects the enhanced CK2 affinity of SGC-CK2-1 versus compound **2**. SGC-CK2-1 is nearly 13-fold more active than compound **2** in the CK2 α ' NanoBRET assay and nearly 26-fold more active than compound **2** in the CK2 α NanoBRET assay.¹¹ Our viability data aligns with literature reports of multiple myeloma survival being impaired via CK2 inhibition.

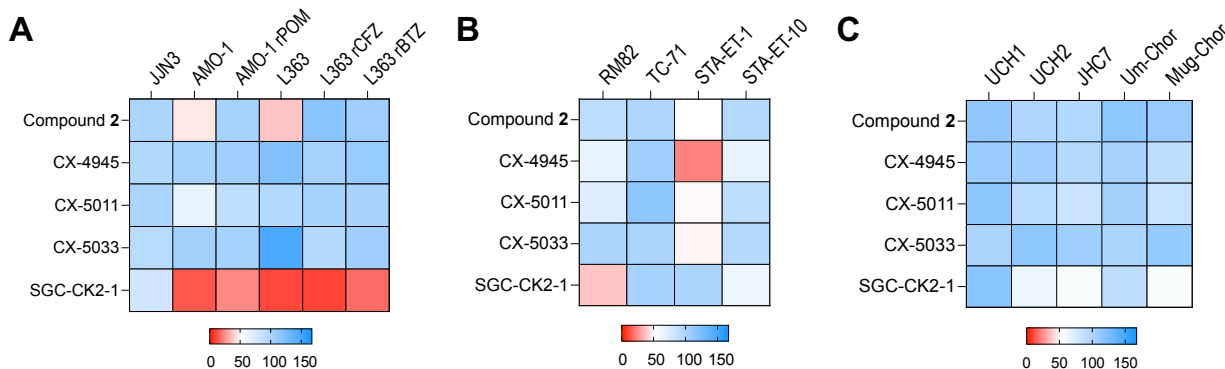


Figure 6. Analysis of impact of naphthyridine analogs and SGC-CK2-1 on viability of (A) multiple myeloma, (B) chordoma, and (C) Ewings sarcoma cell lines when dosed at 1 μ M. Scale bar shows the color gradient that corresponds with percent viability.

Less has been published about the role of CK2 in rare cancers that occur in bones, such as Ewings sarcoma, and in the soft tissue around bones, known as chordoma, a rare slow growing cancer of tissue inside the spine. The *EWS* gene, which encodes a ubiquitously expressed RNA binding protein of the same name, has been identified as a target of tumor-specific translocations in Ewings sarcoma family tumors. A putative CK2 phosphorylation site (Ser325) on an EWS protein isoform has been reported.^{28, 29} Literature links between CK2 and chordoma are tenuous. Validated, repurposed chemotherapeutic drugs have been the focus of most cell-based therapeutic screens related to chordoma.^{30, 31} As an exception, one compound, 5-iodotubericin, that inhibits CK2 in addition to other kinases, has demonstrated dose-responsive inhibition of UCH1 chordoma cells.³² Motivated to explore whether CK2 inhibition is a therapeutic avenue for these rare cancers, we examined the impact of the same panel of CK2 inhibitors, dosed at 1 μ M, on viability of four Ewings sarcoma and five chordoma cell lines. The preliminary data in Figure 6B demonstrates that most Ewings cell lines were non-responsive to treatment with naphthyridine analogs. The exception to this are STA-ET-1 cells, which were modestly impacted by treatment with these compounds. CX-4945 elicited the most robust response of Ewings cell lines for compounds in this structural series, resulting in 21% viability of STA-ET-1 cells and 63% viability of both RM82 and STA-ET-10 cells. SGC-CK2-1, in contrast, only significantly impacted RM82 cells (36% viability) versus other Ewings cell lines evaluated. When considering the preliminary chordoma cell line data in Figure 6C, limited impact on viability was noted. The exception to this trend was observed for SGC-CK2-1, which showed sensitivity of UCH2, JHC7, and Mug-Chor cells to treatment, resulting in 60%, 53%, and 53% viability, respectively. As was observed in the multiple myeloma cell lines, a chemotype-specific response was observed for SGC-CK2-1 versus naphthyridine-based compounds in chordoma cell lines.

We have described the design, synthesis, and biological evaluation of a series of naphthyridines as inhibitors of CK2. Compound **2** emerged as our most optimal probe candidate. Comparison of co-crystal structures solved for compound **2** versus other naphthyridines revealed a key interaction that may drive its CK2 selectivity and informed design of a structurally related

negative control compound (7). Inhibition of downstream signaling without an associated impact on viability was observed when MDA-MB-231 breast cancer cells were treated with compound 2. In contrast, the viability of specific multiple myeloma cell lines was differentially compromised due to treatment with 1 μ M of compound 2, which may be related to different genomic lesions occurring in myeloma, now recognized as main oncogenic drivers in this cancer.³³ Ewings sarcoma and chordoma cell lines were generally not responsive to treatment with compound 2. Like SGC-CK2-1, compound 2 does not seem to be a broadly antiproliferative agent.¹¹ This finding supports the concept that CK2 inhibition is a possible personalized treatment strategy for specific cancers, including multiple myeloma, and deserves further study.

ASSOCIATED CONTENT

Supporting Information

Supplemental figures, tables, and experimental details. This material is available free of charge via the Internet at <http://pubs.acs.org>.

Accession Codes

The PDB accession code for the X-ray co-crystal structure of CK2 α + 2 is 8BGC.

AUTHOR INFORMATION

Corresponding Author

*E-mail: alison.axtman@unc.edu.

ORCID:

Zachary W. Davis-Gilbert: 0000-0002-4070-0832

Andreas Krämer: 0000-0003-3294-2660

James E. Dunford: 0000-0002-9932-4042

Stefanie Howell: 0000-0003-3392-2848

Filiz Senbabaoglu: 0000-0002-1410-2898

Carrow I. Wells: 0000-0003-4799-6792

Tammy M. Havener: 0000-0002-4613-0498

Jeffery L. Smith: 0000-0003-2189-0420

Udo Oppermann: 0000-0001-9984-5342

Mohammad A. Hossain: 0000-0001-8684-8755

David H. Drewry: 0000-0001-5973-5798

Alison D. Axtman: 0000-0003-4779-9932

Notes

The authors declare no competing financial interest.

ACKNOWLEDGMENT

Promega kindly provided constructs for NanoBRET measurements of CK2 α and CK2 α '. The kinome trees in Figures 2 and 4 and the Table of Contents graphic were prepared using the TREEspot kinase interaction mapping software at <http://treespot.discoverx.com>. We thank the Mark Foundation for Cancer Research and the Chordoma Foundations for supporting our efforts related to the rare cancer chordoma. ChemSpace provided synthetic support for our program. We acknowledge the Department of Chemistry Mass Spectrometry Core Laboratory at the

University of North Carolina for assisting with mass spectrometry analyses. Furthermore, we thank the beamline scientists at the Swiss Light Source (PSI) for their great support during data collection.

The Structural Genomics Consortium (SGC) is a registered charity (number 1097737) that receives funds from Bayer AG, Boehringer Ingelheim, the Canada Foundation for Innovation, Eshelman Institute for Innovation, Genentech, Genome Canada through Ontario Genomics Institute [OGI-196], EU/EFPIA/OICR/McGill/KTH/Diamond, Innovative Medicines Initiative 2 Joint Undertaking [EUbOPEN grant 875510], Janssen, Merck KGaA (aka EMD in Canada and USA), Pfizer, the São Paulo Research Foundation-FAPESP, and Takeda. Research in the Oxford laboratory (U.O.) was supported by Cancer Research UK, the LEAN program grant of the Leducq Foundation, Oxford NIHR Biomedical Research Centre, the Oxford Translational Myeloma Centre, and the BMS-Mt Sinai-Oxford Myeloma Single Cell Consortium. J.E.D. is supported by the Oxford NIHR Biomedical Research Centre. Research reported in this publication was supported in part by DoD ALSRP award AL190107, NC Biotechnology Center Institutional Support Grant 2018-IDG-1030, and NIH U24DK116204.

Abbreviations

BSA, bovine serum albumin; DIPEA, *N, N*-diisopropylethylamine; DMSO, dimethyl sulfoxide; ESI, electrospray ionization; HCl, hydrochloric acid; IC₅₀, half maximal inhibitory concentration; K_m, Michaelis constant; LC–MS, liquid chromatography–mass spectrometry; LiOH, lithium hydroxide; NaH, sodium hydride; NanoBRET, bioluminescence resonance energy transfer using NanoLuciferase; nLuc, NanoLuciferase; NMP, *N*-methyl-2-pyrrolidone; NMR, nuclear magnetic resonance; PoC, percent of control; THF, tetrahydrofuran; TMAH, tetramethylammonium hydroxide; v/v, volume for volume; WT, wild-type.

References

- (1) Meggio, F.; Pinna, L. A. One-thousand-and-one substrates of protein kinase CK2? *FASEB J* **2003**, *17* (3), 349–368, DOI: 10.1096/fj.02-0473rev
- (2) Salvi, M.; Sarno, S.; Cesaro, L.; Nakamura, H.; Pinna, L. A. Extraordinary pleiotropy of protein kinase CK2 revealed by weblogo phosphoproteome analysis. *Biochim Biophys Acta* **2009**, *1793* (5), 847–859, DOI: 10.1016/j.bbamcr.2009.01.013
- (3) Rabalski, A. J.; Gyenis, L.; Litchfield, D. W. Molecular pathways: Emergence of protein kinase CK2 (CSNK2) as a potential target to inhibit survival and DNA damage response and repair pathways in cancer cells. *Clin Cancer Res* **2016**, *22* (12), 2840–2847, DOI: 10.1158/1078-0432.Ccr-15-1314
- (4) Nuñez de Villavicencio-Díaz, T.; Rabalski, A. J.; Litchfield, D. W. Protein kinase CK2: Intricate relationships within regulatory cellular networks. *Pharmaceuticals* **2017**, *10* (1), 27, DOI: 10.3390/ph10010027.
- (5) Ahmed, K.; Gerber, D. A.; Cochet, C. Joining the cell survival squad: An emerging role for protein kinase CK2. *Trends Cell Biol* **2002**, *12* (5), 226–230, DOI: 10.1016/S0962-8924(02)02279-1
- (6) Bouhaddou, M.; Memon, D.; Meyer, B.; White, K. M.; Rezelj, V. V.; Correa Marrero, M.; Polacco, B. J.; Melnyk, J. E.; Ulferts, S.; Kaake, R. M.; et al. The global phosphorylation landscape of SARS-CoV-2 infection. *Cell* **2020**, *182* (3), 685–712.e619. DOI: 10.1016/j.cell.2020.06.034

- (7) Yang, X.; Dickmader, R. J.; Bayati, A.; Taft-Benz, S. A.; Smith, J. L.; Wells, C. I.; Madden, E. A.; Brown, J. W.; Lenarcic, E. M.; Yount, B. L.; et al. Host kinase CSNK2 is a target for inhibition of pathogenic SARS-like β -coronaviruses. *ACS Chem Biol* **2022**, 1937–1950, DOI: 10.1021/acscchembio.2c00378
- (8) Mishra, S.; Kinoshita, C.; Axtman, A. D.; Young, J. E. Evaluation of a selective chemical probe validates that CK2 mediates neuroinflammation in an hiPSC-derived microglial model. *Front Mol Neurosci* **2022**, 15, 824956, DOI: 10.3389/fnmol.2022.824956
- (9) Zakharia, K.; Miyabe, K.; Wang, Y.; Wu, D.; Moser, C. D.; Borad, M. J.; Roberts, L. R. Preclinical in vitro and in vivo evidence of an antitumor effect of CX-4945, a casein kinase II inhibitor, in cholangiocarcinoma. *Transl Oncol* **2019**, 12 (1), 143–153, DOI: 10.1016/j.tranon.2018.09.005
- (10) Chon, H. J.; Bae, K. J.; Lee, Y.; Kim, J. The casein kinase 2 inhibitor, CX-4945, as an anti-cancer drug in treatment of human hematological malignancies. *Front Pharmacol* **2015**, 6, 70, DOI: 10.3389/fphar.2015.00070
- (11) Wells, C. I.; Drewry, D. H.; Pickett, J. E.; Tjaden, A.; Krämer, A.; Müller, S.; Gyenis, L.; Menyhart, D.; Litchfield, D. W.; Knapp, S.; et al. Development of a potent and selective chemical probe for the pleiotropic kinase CK2. *Cell Chem Biol* **2021**, 28, 546–558.e510, DOI: 10.1016/j.chembiol.2020.12.013
- (12) Krämer, A.; Kurz, C. G.; Berger, B.-T.; Celik, I. E.; Tjaden, A.; Greco, F. A.; Knapp, S.; Hanke, T. Optimization of pyrazolo[1,5-a]pyrimidines lead to the identification of a highly selective casein kinase 2 inhibitor. *Eur J Med Chem* **2020**, 208, 112770, DOI: 10.1016/j.ejmech.2020.112770
- (13) Raaf, J.; Bischoff, N.; Klopffleisch, K.; Brunstein, E.; Olsen, B. B.; Vilk, G.; Litchfield, D. W.; Issinger, O.-G.; Niefind, K. Interaction between CK2 α and CK2 β , the subunits of protein kinase CK2: Thermodynamic contributions of key residues on the CK2 α surface. *Biochemistry* **2011**, 50 (4), 512–522, DOI: 10.1021/bi1013563
- (14) Siddiqui-Jain, A.; Drygin, D.; Streiner, N.; Chua, P.; Pierre, F.; O'Brien, S. E.; Bliesath, J.; Omori, M.; Huser, N.; Ho, C.; et al. CX-4945, an orally bioavailable selective inhibitor of protein kinase CK2, inhibits prosurvival and angiogenic signaling and exhibits antitumor efficacy. *Cancer Res* **2010**, 70 (24), 10288–10298, DOI: 10.1158/0008-5472.can-10-1893
- (15) Gowda, C.; Sachdev, M.; Muthusami, S.; Kapadia, M.; Petrovic-Dovat, L.; Hartman, M.; Ding, Y.; Song, C.; Payne, J. L.; Tan, B. H.; et al. Casein kinase II (CK2) as a therapeutic target for hematological malignancies. *Curr Pharm Des* **2017**, 23 (1), 95–107, DOI: 10.2174/1381612822666161006154311
- (16) Pierre, F.; Chua, P. C.; O'Brien, S. E.; Siddiqui-Jain, A.; Bourbon, P.; Haddach, M.; Michaux, J.; Nagasawa, J.; Schwaebe, M. K.; Stefan, E.; et al. Discovery and SAR of 5-(3-chlorophenylamino)benzo[c][2,6]naphthyridine-8-carboxylic acid (CX-4945), the first clinical stage inhibitor of protein kinase CK2 for the treatment of cancer. *J Med Chem* **2011**, 54 (2), 635–654, DOI: 10.1021/jm101251q
- (17) Battistutta, R.; Cozza, G.; Pierre, F.; Papinutto, E.; Lolli, G.; Sarno, S.; O'Brien, S. E.; Siddiqui-Jain, A.; Haddach, M.; Anderes, K.; et al. Unprecedented selectivity and structural determinants of a new class of protein kinase CK2 inhibitors in clinical trials for the treatment of cancer. *Biochemistry* **2011**, 50 (39), 8478–8488, DOI: 10.1021/bi2008382
- (18) Gray, G. K.; McFarland, B. C.; Rowse, A. L.; Gibson, S. A.; Benveniste, E. N. Therapeutic CK2 inhibition attenuates diverse prosurvival signaling cascades and decreases cell viability in human breast cancer cells. *Oncotarget* **2014**, 5 (15), 6484–6496, DOI: 10.18632/oncotarget.2248

- (19) Al Quobaili, F.; Montenarh, M. CK2 and the regulation of the carbohydrate metabolism. *Metab Clin Exp* **2012**, *61* (11), 1512–1517, DOI: 10.1016/j.metabol.2012.07.011
- (20) D'Amore, C.; Moro, E.; Borgo, C.; Itami, K.; Hirota, T.; Pinna, L. A.; Salvi, M. “Janus” efficacy of CX-5011: CK2 inhibition and methuosis induction by independent mechanisms. *Biochim Biophys Acta - Mol Cell Res* **2020**, *1867* (11), 118807. DOI: 10.1016/j.bbamcr.2020.118807
- (21) D'Amore, C.; Borgo, C.; Sarno, S.; Salvi, M. Role of CK2 inhibitor CX-4945 in anti-cancer combination therapy – potential clinical relevance. *Cell Oncol* **2020**, *43* (6), 1003–1016, DOI: 10.1007/s13402-020-00566-w
- (22) Lertsuwan, J.; Lertsuwan, K.; Sawasdichai, A.; Tasnawijitwong, N.; Lee, K. Y.; Kitchen, P.; Afford, S.; Gaston, K.; Jayaraman, P. S.; Satayavivad, J. CX-4945 induces methuosis in cholangiocarcinoma cell lines by a CK2-independent mechanism. *Cancers* **2018**, *10* (9), DOI: 10.3390/cancers10090283
- (23) Li, Z.; Mbah, N. E.; Overmeyer, J. H.; Sarver, J. G.; George, S.; Trabbic, C. J.; Erhardt, P. W.; Maltese, W. A. The JNK signaling pathway plays a key role in methuosis (non-apoptotic cell death) induced by MOMIPP in glioblastoma. *BMC Cancer* **2019**, *19* (1), 77, DOI: 10.1186/s12885-019-5288-y
- (24) Manni, S.; Carrino, M.; Piazza, F. Role of protein kinases CK1 α and CK2 in multiple myeloma: regulation of pivotal survival and stress-managing pathways. *J Hematol Oncol* **2017**, *10* (1), 157, DOI: 10.1186/s13045-017-0529-5
- (25) Ho, C.; Rice, R.; Drygin, D.; Bliesath, J.; Streiner, N.; Siddiqui-Jain, A.; Proffitt, C.; O'Brien, S.; Anderes, K. CX-4945, a selective and orally bioavailable inhibitor of protein kinase CK2 inhibits PI3K/Akt, JAK-STAT and NF- κ B signaling and induces apoptosis in multiple myeloma cells. *Blood* **2010**, *116* (21), 787–787, DOI: 10.1182/blood.V116.21.787.787
- (26) Piazza, F. A.; Ruzzene, M.; Gurrieri, C.; Montini, B.; Bonanni, L.; Chioetto, G.; Di Maira, G.; Barbon, F.; Cabrelle, A.; Zambello, R.; et al. Multiple myeloma cell survival relies on high activity of protein kinase CK2. *Blood* **2006**, *108* (5), 1698–1707, DOI: 10.1182/blood-2005-11-013672
- (27) Piazza, F. A.; Gurrieri, C.; Trentin, L.; Semenzato, G. Towards a new age in the treatment of multiple myeloma. *Ann Hematol* **2007**, *86* (3), 159–172, DOI: 10.1007/s00277-006-0239-5
- (28) Kovar, H.; Jug, G.; Hattinger, C.; Spahn, L.; Aryee, D. N. T.; Ambros, P. F.; Zoubek, A.; Gadner, H. The EWS protein is dispensable for Ewing tumor growth. *Cancer Res* **2001**, *61* (16), 5992–5997
- (29) Paronetto, M. P. Ewing sarcoma protein: A key player in human cancer. *Int J Cell Biol* **2013**, *2013*, 642853, DOI: 10.1155/2013/642853
- (30) Bayrak, O. F.; Aydemir, E.; Gulluoglu, S.; Sahin, F.; Seveli, S.; Yalvac, M. E.; Acar, H.; Ozen, M. The effects of chemotherapeutic agents on differentiated chordoma cells. *J Neurosurg Spine* **2011**, *15* (6), 620–624, DOI: 10.3171/2011.7.Spine10798
- (31) Xia, M.; Huang, R.; Sakamuru, S.; Alcorta, D.; Cho, M. H.; Lee, D. H.; Park, D. M.; Kelley, M. J.; Sommer, J.; Austin, C. P. Identification of repurposed small molecule drugs for chordoma therapy. *Cancer Biol Ther* **2013**, *14* (7), 638–647, DOI: 10.4161/cbt.24596
- (32) Ricci-Vitiani, L.; Runci, D.; D'Alessandris, Q. G.; Cenci, T.; Martini, M.; Bianchi, F.; Maira, G.; Stancato, L.; De Maria, R.; Larocca, L. M.; et al. Chemotherapy of skull base chordoma tailored on responsiveness of patient-derived tumor cells to rapamycin. *Neoplasia* **2013**, *15* (7), 773–782, DOI: 10.1593/neo.13150

(33) Kumar, S. K.; Rajkumar, V.; Kyle, R. A.; van Duin, M.; Sonneveld, P.; Mateos, M.-V.; Gay, F.; Anderson, K. C. Multiple myeloma. *Nat Rev Dis Primers* **2017**, 3 (1), 17046, DOI: 10.1038/nrdp.2017.46

For Table of Contents Only

